DYNAMIC SIMULATION OF LARGE WIND FARMS INTEGRATED IN A MULTI MACHINE NETWORK

F. W. Koch, I. Erlich, *Member, IEEE,* and F. Shewarega

Abstract-- **With the increased use of wind power, particularly in wind-farms, the voltage and frequency behaviors of the whole network are likely to be affected significantly. This paper presents simulation results calculated using a representative network containing wind power generations of up to 30%. Furthermore, modelling and simulation of different types of wind generators integrated into a multi-machine power system are discussed. Special interest is focused on the doubly-fed induction machine, whose primary control structure comprises of decoupled active and reactive power control channels. The overall control schema also includes power, speed and voltage control loops, which provide the reference values for active and reactive power. It is shown that with a simple extension of the control structure, wind generators can participate on the network frequency control and thus are able to reduce the adverse effects of the wind farms on the overall performance of the network.**

Index Terms-- **Digital Control, Frequency Control, Power System Control, Power System Modeling, Variable Speed Drives, Voltage Control, Wind Power Generation.**

I. NOMENCLATURE

A_R	Swept area
c_p	Power coefficient
H	Time-discrete control-matrix
h	Time-discrete disturbance-matrix
I	Unit matrix
$\underline{i}$	Complex current
k	Sampling step
l_h	Main-field inductance
l	Inductance
m_W	Torque of turbine-shaft
R	Controller matrix
r	Resistance
T_m	Inertia constant
u	Voltage phasor
v_W	Wind speed
x, $c_{1..6}$	Parameters emanating from rotor geometry
y	Output of the regulator
α	Pitch angle
λ	Tip speed ratio
ρ	Air density
$\mathbf{\Phi}$	Discrete transition matrix
$\underline{\Psi}$	Complex flux-linkage
$\mathbf{\Psi}$	Vector of flux- linkage
ω_K	Angular velocity of the reference frame
ω_b	Asynchronous angular velocity

Superscripts and subscripts

*	Reference values
S, R	Stator, rotor
d, q	Direct, quadrature axis component

F. W. Koch, University of Duisburg, Germany, (e-mail: friedrich.koch@uni-duisburg.de).
I. Erlich, University of Duisburg, Germany, (e-mail: erlich@uni-duisburg.de).
F. Shewarega, University of Duisburg, Germany, (e-mail: shewarega@uni-duisburg.de).

II. INTRODUCTION

THE reduction of CO_2 emission achieved by the utilisation of the wind energy in the last years on the one hand and the difficulty of finding suitable additional spaces onshore on the other hand makes offshore wind farms (OWF) an interesting alternative. Another reason for the choice of offshore locations is the fact that wind speeds offshore are considerably higher and more uniform compared to onshore sites. Therefore, it is expected that wind farms of several hundreds of MW capacity will be connected to the European grids in the coming years.

Consequently, the impact of these wind farms on the overall system performance will increase and it is likely that the OWF will significantly affect the performance indices of the interconnected system. This circumstance requires an extensive analysis of the interactions of the anticipated OWF with the existing systems.

The salient feature of a wind plant (offshore or onshore) is the inherently stochastic nature of the input mechanical power. With the increase in the share of the wind power, the capability of the wind farms to affect the system performance (positively or adversely) increases correspondingly. As a result, the following questions arise now: Should the OWF be involved in the regulation of the overall system to which they are connected? If so, what are the viable options?

The objective of this paper is, therefore, to study alternative machine types and their control strategies with regard to their steady-state and dynamic behaviour in particular and their overall influence on the power system on which they are operating in general with special regard to the stochastic nature of the wind power.

0-7803-7989-6/03/$17.00 ©2003 IEEE

The paper is structured as follows. In the following chapter basic relationships pertaining to the use of wind power for electricity generation and its modeling (with emphasis on the electrical side) will be briefly reviewed. Then, the proposed control scheme will be elaborated. Finally, results obtained by applying the algorithm on a realistic test network will be presented and discussed.

III. WIND TURBINE MODELING

Wind turbines, which may be used in conjunction with fixed or variable speed generators, are generally classified as stall-type or pitch-controlled. This fact in turn has a significant bearing on the type of control scheme to be adopted for the generator.

The induction machine operating as a generator is a commonly used energy conversion device. In the following sections three alternative set-ups will be considered: a stall turbine operating on a squirrel-cage induction machine (STALL-SCIM), a pitch-controlled turbine again operating on a squirrel-cage induction machine (PITCH-SCIM) and a pitch-controlled turbine operating on a doubly-fed slip-ring induction machine (PITCH-DFIM).

A. Aerodynamic/mechanical energy conversion

In the aerodynamic/mechanical energy conversion mechanism the wind turbine output power is described by the equations (1) and (2)

$$P_W = \frac{\rho}{2} c_p(\lambda,\alpha) A_R v_W^3 \tag{1}$$

$$c_p(\lambda,\alpha) = c_1\left(c_2 - c_3\alpha - c_4\alpha^x - c_5\right)e^{-c_6(\lambda,\alpha)} \tag{2}$$

For further details on (1) and (2), the reader may be referred to [1], where additional information on the relevant parameters of the stall and pitch-controlled wind turbine models used in this paper can be found.

B. Mechanical/electrical energy conversion

Relationships describing the mechanical/electrical energy conversion process using the induction machine are given by equations (3)-(7)

$$\underline{u}_S^{\angle K} = r_S \underline{i}_S^{\angle K} + \frac{d\underline{\psi}_S^{\angle K}}{dt} + j\omega_K \underline{\psi}_S^{\angle K} \tag{3}$$

$$\underline{u}_R^{\angle K} = r_R \underline{i}_R^{\angle K} + \frac{d\underline{\psi}_R^{\angle K}}{dt} + j(\omega_K - \omega_R)\underline{\psi}_R^{\angle K} \tag{4}$$

$$\underline{\psi}_S^{\angle K} = l_S \underline{i}_S^{\angle K} + l_h \underline{i}_R^{\angle K} \tag{5}$$

$$\underline{\psi}_R^{\angle K} = l_h \underline{i}_S^{\angle K} + l_R \underline{i}_R^{\angle K} \tag{6}$$

$$\frac{d\omega_R}{dt} = \frac{1}{T_m}\left(m_W + \psi_{Sd} i_{Sq} - \psi_{Sq} i_{Sd}\right) \tag{7}$$

In the above equations, per unit quantities are used, and $\angle K$ stands for an arbitrary rotating reference frame.

Neglecting the stator transients and after a series of substitutions, which are discussed in [2] and [3], the equations are brought to a state space form in (8) with the resulting relationship for the rotor flux linkages $\underline{\psi}_R^{\angle K}$ as state variables and the stator and rotor voltages, $\underline{u}_S^{\angle K}$ and $\underline{u}_R^{\angle K}$, respectively, as input variables.

$$\frac{d\underline{\psi}_R^{\angle K}}{dt} = -(\underline{T}_{L0}^{-1} + j\frac{\omega_0 k_R^2 r_R}{\underline{z}})\underline{\psi}_R^{\angle K} + \frac{r_R k_R}{\underline{z}}\underline{u}_S^{\angle K} + \underline{u}_R^{\angle K} \tag{8}$$

The nomenclature of the constants and variables used in (8) is provided at the beginning of the paper.

The complex rotor voltage $\underline{u}_R^{\angle K}$ is zero for the SCIM, and for the DFIM a variable $\underline{u}_R^{\angle K}$ is provided by the converter. Attention should be drawn to this feature of the DFIM, which –with the controlled variation of the real and imaginary components of this voltage- enables a decoupled control of the active and reactive power outputs of the machine. This increases the control variability of the DFIM compared to the SCIM.

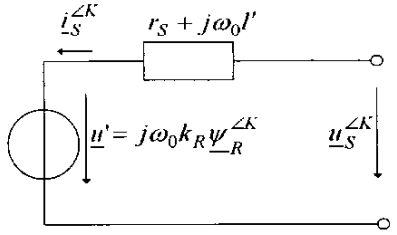

Fig. 1. Equivalent circuit of a DFIM

The stator current is used as a coupling variable with the network equations (as depicted in Fig. 1), and the driving voltage behind the transient reactance is calculated from the rotor flux linkages.

Finally, the differential equation of motion can be given in the following form.

$$\frac{d\omega_R}{dt} = \frac{1}{T_m}\left(m_W + k_R \cdot \left(\psi_{Rd} i_{Sq} - \psi_{Rq} i_{Sd}\right)\right) \tag{9}$$

C. Control System

The mechanical power output of a wind turbine depends on the wind speed and the pitch angle.

As the wind speed varies stochastically, the pitch angle is the only means by which the power output of a wind unit can be controlled continuously. The control approach is fairly straightforward. The pitch angle is normally adjusted for maximum output except under conditions of wind over-speed during which the output power is limited to the rated value by the pitch angle control.

Maintaining a reserve power for control purpose at any given wind unit operating on an interconnected system necessitates the adjustment of the pitch angle for an output less than what normally would have been possible. The balance is the reserve power available for frequency control.

The pitch angle in a stall-controlled turbine is fixed. The rotor is designed in such a way that it stalls at wind over-speed thereby protecting the turbine from mechanical damage.

Within the normal range of wind speeds, the power generation is determined by the actual wind speed.

The output power of a SCIM depends on the slip. The slip, however, varies only over a small margin for the normal operational range of the machine.

The DFIM is a slip-ring induction machine with the rotor windings connected to a variable frequency supply provided by a converter operating on the grid. By varying the frequency of the rotor voltage, the rotor speed and with it the generated power can be varied. In addition, the amplitude of $\underline{u}_R^{\angle K}$ can be modified independently. With these two variables (frequency and amplitude of rotor voltage) a decoupled control of the real and reactive power outputs is possible. The procedure resembles the principle of field-oriented control. However, in the discussions to follow a distinct approach based on a systematic design of a multivariable controller will be presented, which achieves a similar result [4].

For the derivation of the algorithms for the electronic control system of the PITCH-DFIM, the state equation (8) was transformed into the time-discrete vector form.

$$\boldsymbol{\Psi}_R^{\angle K}(k+1) = \boldsymbol{\Phi}(\omega_R, \omega_K) \cdot \boldsymbol{\Psi}_R^{\angle K}(k) + \mathbf{H} \cdot \mathbf{u}_R^{\angle K}(k) + \mathbf{h} \cdot \mathbf{u}_S^{\angle K}(k) \quad (10)$$

The control basic approach

$$\mathbf{u}_R^{\angle K}(k) = \mathbf{H}^{-1} \cdot \left(\mathbf{y}^{\angle K}(k-1) - \mathbf{h} \cdot \mathbf{u}_S^{\angle K}(k)\right) \quad (11)$$

results in

$$\boldsymbol{\Psi}_R^{\angle K}(k+1) - \boldsymbol{\Phi}(\omega_R, \omega_K) \cdot \boldsymbol{\Psi}_R^{\angle K}(k) = \mathbf{y}^{\angle K}(k-1) \quad (12)$$

or in z-plane

$$(z\mathbf{I} - \boldsymbol{\Phi}) \cdot \boldsymbol{\Psi}_R^{\angle K}(z) = z^{-1} \cdot \mathbf{y}^{\angle K}(z) \quad (13)$$

In a multi-machine network, the stator terminal voltage is not constant. In the state equations, it appears as a disturbance variable, which can be eliminated using the control equation (11). The exact elimination of $\underline{u}_S^{\angle K}$ would have been possible for known value of $\underline{u}_S^{\angle K}(k+1)$, i.e. for the next sampling point, which, of course, is not the case. However, a prediction of $\underline{u}_S^{\angle K}(k+1)$ using a linear extrapolation with sufficient accuracy is possible [5].

Finally, the control equation is formulated as follows:

$$\mathbf{y}^{\angle K}(z) = \mathbf{R} \cdot (\boldsymbol{\Psi}_R^{\angle K^*}(z) - \boldsymbol{\Psi}_R^{\angle K}(z)) \quad (14)$$

$\mathbf{R}$ is the place holder for a controller to be implemented. In this study a controller with dead-beat behaviour has been used.

The reference values for rotor flux linkages, $\boldsymbol{\Psi}_R^{\angle K^*}$, can be calculated from power reference values. The corresponding relationships can be derived from the equivalent circuit (Fig. 1).

The model discussed up to this point will be referred to as the inner control loop. The reference values for the active and reactive power will be provided by the controllers in the outer loop. The outer control loop consists of the active power and voltage controllers as shown in Fig.2.

In addition to these fast-acting electronic control circuits, the overall control scheme includes the mechanical pitch angle control, which is the speed control in the DFIM and the power control in the Pitch SCIM.

For the investigation of alternative control options, the control scheme in Fig. 2 is extended by a block for network frequency control. This version is referred to as PITCH-DFIM+FR in this paper.

Participation of the wind unit in the network frequency control presupposes a power reserve that can be called upon when the need arises. To emphasize the obvious, the unit needs to be adjusted so as to utilize only part of the wind power yield and to forgo the rest to be maintained as a reserve.

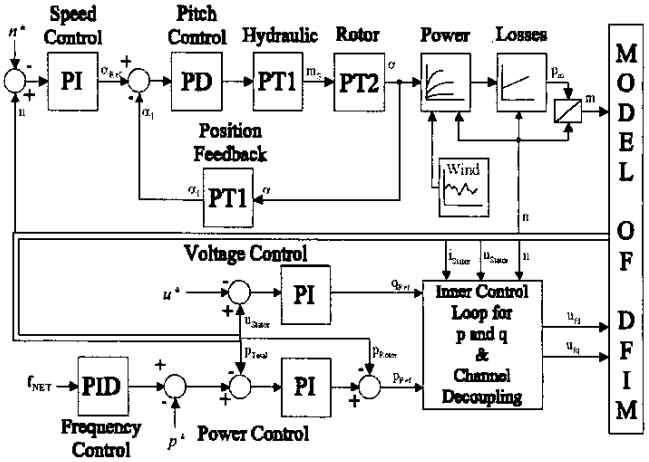

Fig. 2. General Control Scheme of Pitch-DFIM+FR

IV. SIMULATION OF THE ENTIRE SYSTEM

For the investigation of the dynamic behaviour of a power system, which includes wind farms and conventional plants operating in synchronism, the proposed models and the control systems were incorporated into the package PSD (Power System Dynamics).

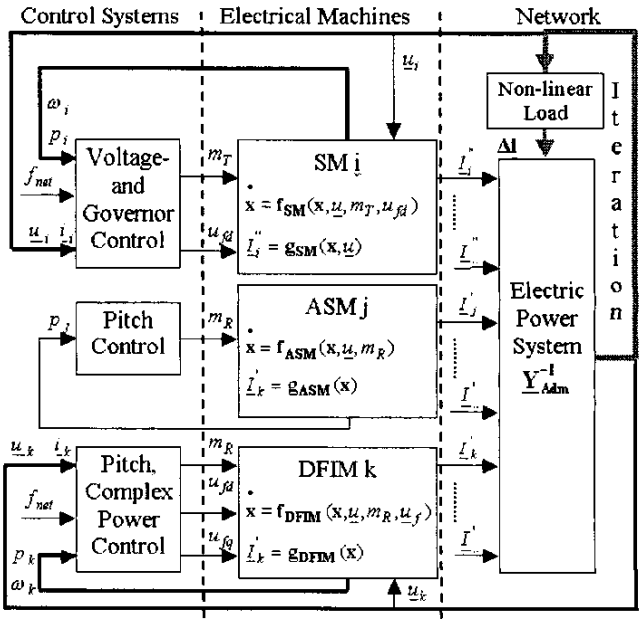

Fig. 3. Structure of the Simulation Model

PSD is a program system with a wide array of capabilities, including steady-state analysis of power systems and the analysis of various aspects of power system dynamics.
Fig. 3 describes the overall structure of PSD with emphasis on the modelling of wind converters and their control gear.

TABLE I
LIST OF COMPONENTS OF THE PST16

COMPONENT	QUANTITY
Generation units	16
2-Winding Transformation units	16
3-Winding Transformation units	12
Bus-Bars	66
Transmission lines	51

The test network used for the simulations in this study is presented on Fig. 4 and Table 1. For further details concerning the test network [6], the reader is invited to visit the website given in the Reference section

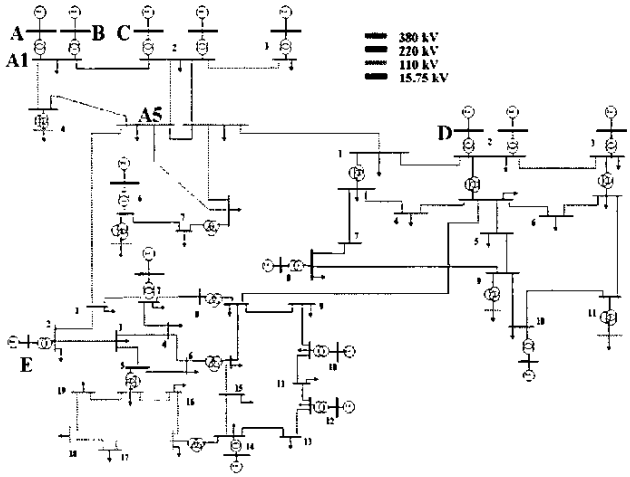

Fig. 4. Power Simulation Test network (PST16)

V. SIMULATION RESULTS

In the study, five wind units connected to the test network PST16 at five different locations were simulated. The exact locations are shown in Table 2. The time behaviour of the system in terms of frequency variations and voltage profile for varying power outputs of the wind farms with a simultaneous decrease of power outputs in the conventional plants was observed. An additional point of interest was the reaction of conventional power plants to network frequency fluctuations caused by the wind park in-feed.
In case 1, the wind farm 1 (at position A) with the initial power output of 1 GW (6% of the overall system power) replaces a conventional power plant of the same output and at the same location.
In the subsequent cases, this process is repeated in all the different locations given in Table 2 and shown in Fig. 4. At the end of the final step, five wind farms with a combined output of 5 GW (30% of the total) are connected to the system.

The simulation was carried out for a time interval ranging 2.5 minutes. This time range is deemed to be sufficient for observing the impact of the changes on the primary control of the conventional generators in full.

TABLE II
FIVE ALTERNATIVE SCENARIOS INVESTIGATED

CASE	TOTAL WIND POWER	POSITION IN PST16
1	1 x 1 GW (6 % of P_{Net})	A
2	2 x 1 GW (12 % of P_{Net})	A, B
3	3 x 1 GW (18 % of P_{Net})	A, B, C
4	4 x 1 GW (24 % of P_{Net})	A, B, C, D
5	5 x 1 GW (30 % of P_{Net})	A, B, C, D, E

A. *Effect of wind power on the system frequency*

Figures 5 (a, b, c) summarise the results of the simulation for different turbine types.

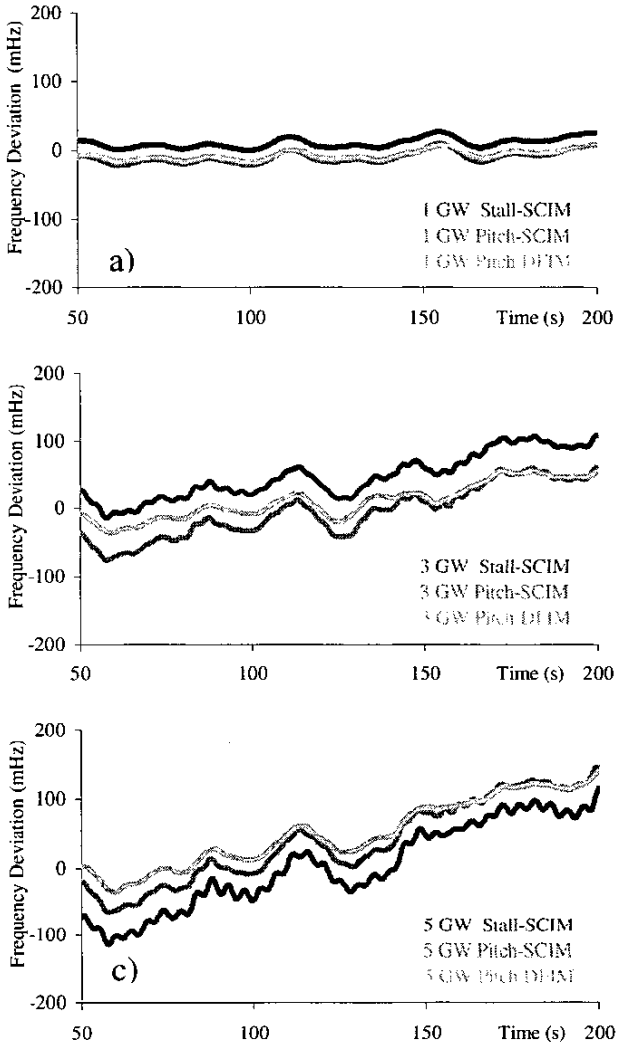

Fig. 5. Frequency excursions in the network with increasing wind power

The curves show that the frequency deviation Δf rises with the increase in the contribution of the wind farms for all three turbine types. In this example, for the combined wind farm outputs of 1 GW, 3 GW and 5 GW the maximum frequency

excursions experienced in the observed 2.5 minutes are listed in Table 3.

With regard to their steady-state performance in relation to frequency, the three turbine types exhibit a similar characteristic. With the DFIM, a degree of smoothing of the frequency excursion is observed.

TABLE III
FREQUENCY EXCURSIONS OF THE VARIOUS ASYNCHRONOUS MACHINE TYPES

TYPE	Δf/mHz FOR AN OUTPUT OF:		
	1 GW	3 GW	5 GW
Stall-SCIM	26.4	124	230
Pitch-SCIM	31.1	138	212
Pitch-DFIM	24.1	94	174

The stochastic nature of the wind speed leads to a continuous power mismatch, which wobbles with the share of the wind power in the overall power output of the system. The conventional power plants are constantly called upon to off-set this power mismatch. It should be emphasised that in spite of the intervention by the conventional plants, the frequency deviations depicted in Fig. 5 are observed.

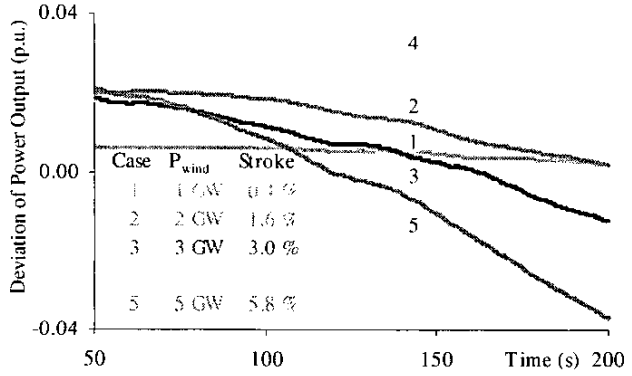

Fig. 6. Excursion of power output in conventional plants

The necessary change in the output of one of the conventional plants (denoted as stroke) to even out the discrepancy is given in Fig. 6. This scenario represents the most favourable case as a Pitch-DFIM, which causes the lowest frequency deviation, was used. The DFIM is chosen in this example merely due to the fact that it is to be pursued further in the next section in connection with the frequency control option.

B. Effect of the OWF frequency control

It follows from the discussions in the preceding sections that large wind power feeding in an interconnected system leads to frequency wobbling. The larger the share of the wind power, the more pronounced this phenomenon becomes.

The current practice is to leave the task of frequency maintenance to the conventional plants. As the results of this study will demonstrate, the wind farms themselves can contribute towards the alleviation of the problem of frequency fluctuation arising from the increase of the share of the wind power. For this purpose, the wind turbine needs to be equipped with a frequency and a pitch control, which maintains a reserve power. The reserve power can then be used to reduce frequency deviation in combination with the frequency control.

Fig. 7 compares the frequency deviation in a Pitch-DFIM shown earlier in Fig. 5c with a Pitch-DFIM+FR with a 4% power reserve. In the latter case, the frequency deviation was reduced from 174 mHz to 28 mHz.

The increased involvement of the wind turbines in maintaining the frequency obviously relieves the pressure on the primary control of the conventional plants. This is demonstrated in Fig. 8.

As can be seen in Fig. 6, for a 30% (5 GW) share of the wind power in the overall power generation, the stroke is found to be 5.8%. In Fig. 8 this same situation is represented in comparison with the Pitch-DFIM+FR. The difference turns out to be significant. In addition to the reduced frequency deviation described in Fig. 7, the stroke is reduced to a mere 1.5%.

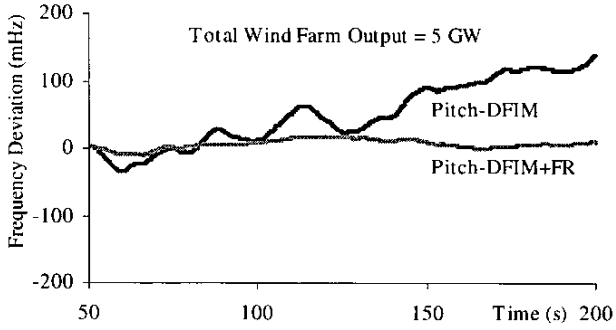

Fig. 7. Network frequency deviations with and without frequency control of DFIM

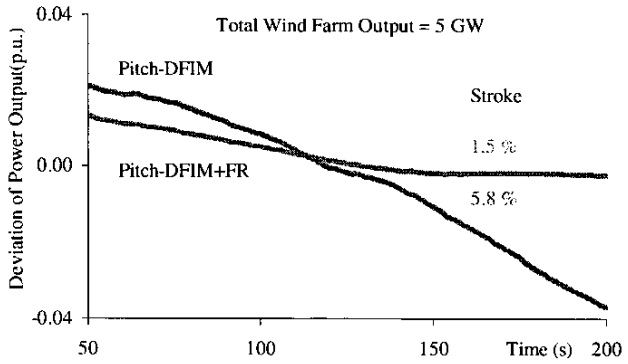

Fig. 8. Excursion of output in conventional plants with and without frequency control of DFIM

C. Voltage control

A further point of interest in the study was the effect of the turbine types on the voltage profile of the network. For this purpose, the combined output of the wind farms was set at 5 GW (30% of the total). The voltage magnitudes were then observed at a bus directly connected to a wind farm (A1) and at an intermediate location (A5). The distance between the two buses considered is about 150 km (length of the transmission line).

The voltages at the two buses in relation to the type of machines used are given in Fig. 9 for bus A1 and in Fig. 10

for bus A5. At bus A1, which is directly connected to a wind farm, the maximum voltage deviation for the SCIM is about 1.5%, which occurs at the maximum wind power generation. However, Fig. 9 reveals that the wind power generation in SCIM excites the system to an un-damped electromechanical oscillation. This behaviour is not acceptable in system operation and requires corresponding counter measures. The DFIM on the other hand demonstrates a nearly constant voltage characteristic.

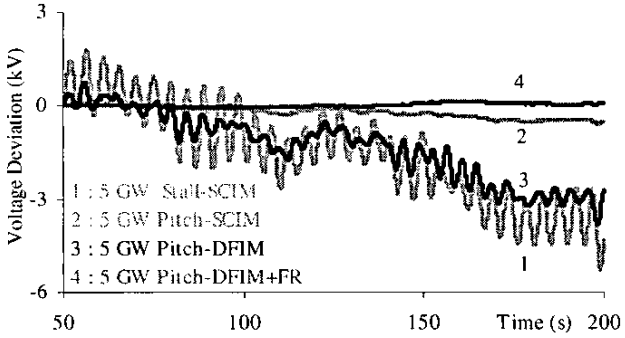

Fig. 10. Voltage characteristics at Bus A1

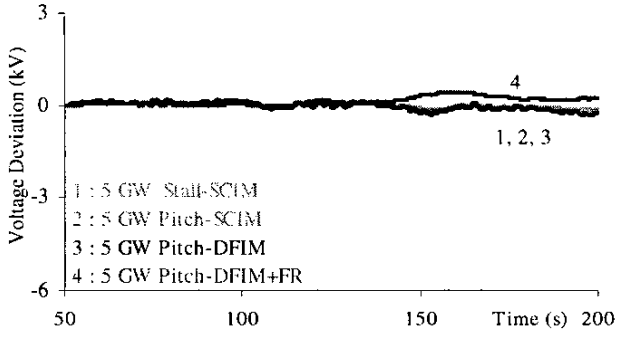

Fig. 10. Voltage characteristics at Bus A5

VI. CONCLUSION

As the share of the wind power in the system increases, the frequency fluctuations will increase significantly. Without counter measure, this frequency deviation can attain unacceptable values. Furthermore, the wind farms affect the voltage behaviour adversely. Although the mean voltage drop is not as significant as that of the frequency deviation, the SCIM wind converters cause electromechanical oscillations, which are undesirable in power system operation. DFIM converters lead to a much better behaviour due to their fast voltage and power control capabilities.

The primary control in the conventional plants are repeatedly required to respond to the fluctuating wind power in-feed. Therefore, the necessary control power will increase.

In the paper an approach has been proposed in which the OWF are integrated into the overall frequency control regime. Results obtained on a test network demonstrate that the adverse effects of wind power on the performance indices of the interconnected system can be reduced significantly.

In conclusion, it should be emphasised that the wind farms, in accordance with costs-by-cause principle, can help ameliorate the problem themselves.

VII. REFERENCES

[1] Slootweg J. G.; Polinder H.; Kling W.L.: Initialization of Wind Turbine Models in Power System Dynamics Simulations, IEEE Porto Power Tech Conference, 2001.

[2] Erlich, I.: Analysis and Simulation of the Dynamic Behavior of Electrical Power Systems, Habilitation-Thesis, Technical University of Dresden, Department of Electrical Engineering, 1995.

[3] Kundur, P.: Power System Stability and Control, McGraw-Hill, ISBN 0-07-035958-X, 1994.

[4] Erlich, I.; Bachmann, U.: Dynamic Behavior of Variable Speed Pump Storage Units in the German Electric Power System, IFAC 15th Triennial World Congress, Barcelona, Spain, 2002.

[5] Grotenburg, K.; Koch, F.; Erlich, I.; Bachmann, U.: Modeling and Dynamic Simulation of Variable Speed Pump Storage Units Incorporated into the German Electric Power System, EPE Congress, Graz, Austria, 2001.

[6] www.uni-duisburg.de/FB9/EAN/doku/teeuwsen/PST16.html

VIII. APPENDIX

All equations are based on the load reference arrow system.

$$\underline{T}_{L0}^{-1} = \frac{r_R}{l_h + l_R} + j(\omega_K - \omega_R) \tag{A1}$$

$$\underline{z}' = r_S + j\omega_0 l' \tag{A2}$$

$$k_R = \frac{l_h}{l_h + l_R} \tag{A3}$$

$$l' = l_h + l_S - \frac{l_h^2}{l_h + l_R} \tag{A4}$$

IX. BIOGRAPHIES

Friedrich W. Koch (1969) is presently PhD student in the Department of Electrical Power Systems at the University of Duisburg/Germany. He received his Dipl.-Ing. degree in electrical engineering from the University of Siegen/Germany in 1998. After his studies, he worked in the field of industrial- and power plants. He is a member of VDE.

Istvan Erlich (1953) received his Dipl.-Ing. degree in electrical engineering from the University of Dresden/Germany in 1976. After his studies, he worked in Hungary in the field of electrical distribution networks. From 1979 to 1991, he joined the Department of Electrical Power Systems of the University of Dresden again, where he received his PhD degree in 1983. In the period of 1991 to 1998, he worked with the consulting company EAB in Berlin and the Fraunhofer Institute IITB Dresden respectively. During this time, he also had a teaching assignment at the University of Dresden. Since 1998, he is Professor and head of the Institute of Electrical Power Systems at the University of Duisburg/Germany. His major scientific interest is focused on power system stability and control, modelling and simulation of power system dynamics including intelligent system applications. He is a member of VDE and IEEE.

Fekadu Shewarega (1956) received his Dipl.-Ing. degree in electrical engineering from the Technical University of Dresden, Germany in 1985. From 1985 to 1988 he pursued his postgraduate studies in the same university and obtained his PhD degree in 1988. After graduation, he joined the Addis Ababa University, Ethiopia as the member of the academic staff where he served in various capacities. His research interests are focussed on power system analysis and rural electrification options.